16

SANDIA REPORT

SAND98–0537 • UC–401
Unlimited Release
Printed March 1998

Two-Dimensional Green's Function Poisson Solution Appropriate for Feature-Scale Microelectronics Simulations

Merle E. Riley

Prepared by
Sandia National Laboratories
Albuquerque, New Mexico 87185 and Livermore, California 94550

Sandia is a multiprogram laboratory operated by Sandia Corporation, a Lockheed Martin Company, for the United States Department of Energy under Contract DE-AC04-94AL85000.

Approved for public release; further dissemination unlimited.

Sandia National Laboratories

Issued by Sandia National Laboratories, operated for the United States Department of Energy by Sandia Corporation.

Available to DOE and DOE contractors from
Office of Scientific and Technical Information
P.O. Box 62
Oak Ridge, TN 37831

Prices available from (615) 576-8401, FTS 626-8401

Available to the public from
National Technical Information Service
U.S. Department of Commerce
5285 Port Royal Rd
Springfield, VA 22161

NTIS price codes
Printed copy: A04
Microfiche copy: A01

SAND98-0537
Unlimited Release
Printed March 1998

Distribution
Category UC-401

Two-Dimensional Green's Function Poisson Solution Appropriate for Feature-Scale Microelectronics Simulations

Merle E. Riley
Laser, Optics, and Remote Sensing Department
Sandia National Laboratories
P.O. Box 5800
Albuquerque, NM 87185-1423

Abstract

This report describes the numerical procedure used to implement the Green's function method for solving the Poisson equation in two-dimensional Cartesian coordinates. The procedure can determine the solution to a problem with any or all of applied voltage boundary conditions, dielectric media, floating (insulated) conducting media, dielectric surface charging, periodic (reflective) boundary conditions, and volumetric space charge. The numerical solution is reasonably fast, and the dimension of the linear problem to be solved is that of the number of elements needed to represent the surfaces, not the whole computational volume. The method of solution is useful in the simulation of plasma particle motion in the vicinity of complex surface structures as found in microelectronics plasma processing applications. A Fortran implementation of this procedure is available from the author.

I. Introduction

The fields about a prescribed distribution of electric charge are solved by superposition once Coulomb's law is introduced. In general though, problems are specified in terms of known voltage boundary conditions, not charge distributions, which requires the solution of partial differential equations or integral equations.[1] Finite difference techniques for solving the Poisson or Laplace equations are standard fare. They require numerical solutions covering the whole computation volume of the problem. An alternative method is to use the Green's function for an unknown source distribution, with sources localized to the surfaces, and to formulate the solution as a Fredholm integral equation of first kind,[2] which becomes a linear algebra problem once discretized. The advantage of the Green's function technique is the smaller dimension of the array of surface unknowns as compared to the number of volume elements filling the whole computation volume. This is illustrated by considering a square of N elements on a side. The Green's function method has 4N unknowns and a 4N by 4N coupling matrix. A finite difference formulation would have N^2 unknowns and a N^2 by N^2 matrix. However the latter matrix is sparse (tridiagonal, perhaps) and numerical methods exist to take advantage of the sparseness.

The Poisson equation (PE) in three dimensions (3D) for the potential field V due to a distribution of charge ρ is

$$\nabla^2 V(\vec{R}) = -\rho(\vec{R}) / \varepsilon_o \tag{1}$$

where SI units are used: namely, distance is in m, V is in volts (V), ρ is in C/m^3, and the vacuum permittivity ε_o is in C^2/J m. The PE can be resolved by use of the free-space Green's function:[1,2]

$$\begin{aligned} G_o(\vec{R},\vec{R}') &= -1/4\pi\left|\vec{R}-\vec{R}'\right|, \\ \nabla_R^2 G_o(\vec{R},\vec{R}') &= \delta^3(\vec{R}-\vec{R}'), \end{aligned} \tag{2}$$

as

$$\begin{aligned} V(\vec{R}) &= -\frac{1}{\varepsilon_o}\int d^3R'\, G_o(\vec{R},\vec{R}')\rho(\vec{R}') \\ &= \int d^3R'\, \rho(\vec{R}')/4\pi\varepsilon_o\left|\vec{R}-\vec{R}'\right|. \end{aligned} \tag{3}$$

The form of G_o is chosen to vanish at large distance analogous to the Coulomb field of a charged particle. Homogeneous solutions of the Laplace equation are not superimposed with the PE particular solution, because all fields are due to, or represented as, the superposition of real charges. This carries over to the representation of dielectric media, which are replaced by charged surfaces rather than a space-dependent permittivity, $\varepsilon(\vec{R})$.

A point of importance in the application of the Poisson solver to plasma physics problems is the stiffness that is associated with the light electron mass and relatively high temperature. This is discussed in the Appendix of this report.

II. The Two-Dimensional Poisson Equation

The 2D PE may be obtained by introducing a restricted spatial dependence into the PE in Eq.(1) or the Green's function solution as given in Eq.(3). This is not completely straightforward due to a divergent integral that occurs when one assumes that the charge distributions extend to $\pm\infty$ in the z coordinate. This can be done in a limiting process, however, and the result is the conversion to 2D coordinates:

$$\begin{aligned} \rho(\vec{R}) &\rightarrow \rho(x,y) \equiv \rho(\vec{r}), \\ V(\vec{R}) &\rightarrow V(x,y) \equiv V(\vec{r}). \end{aligned} \tag{4}$$

Lower case $\vec{r}$ is used to denote a vector in (x,y) space. The new 2D Green's function is[2]

$$\begin{aligned} G(\vec{r},\vec{r}\,') &= (1/2\pi)\ln(r/R_1), \\ r = |\vec{r}-\vec{r}\,'| &\equiv \sqrt{(x-x')^2+(y-y')^2}\,, \\ \left(\frac{\partial^2}{\partial^2 x}+\frac{\partial^2}{\partial^2 y}\right) G(\vec{r},\vec{r}\,') &= \delta(x-x')\delta(y-y') \equiv \delta^2(\vec{r}-\vec{r}\,'), \end{aligned} \tag{5}$$

where R_1 is an arbitrary constant fixing the location of the zero of the potential field about a 2D line source of charge, which is the idealization of a long charged wire. One notes that the 2D Green's function always diverges at both large and small r.

The potential due to a volume distribution of charge is given by

$$V(\vec{r}) = -\frac{1}{\varepsilon_o}\int d^2r'\, G(\vec{r},\vec{r}')\,\rho(\vec{r}'). \qquad (6)$$

Of course this distribution and potential are uniform in the z coordinate. In the case that a surface charge is present, say $\sigma(\vec{r})$, in units of C/m^2, the appropriate potential is given by taking a zero-thickness or surface-delta-function limit of a volume charge. Let t be the local coordinate normal to the surface, which is located at t_s, then the substitution of

$$\rho(\vec{r}) = \sigma(\vec{r})\,\delta(t - t_s) \qquad (7)$$

will convert the volume charge integration to a surface integration. The solution to the surface-charge problem is represented as the 1D integral covering all surfaces:

$$V(\vec{r}) = -\frac{1}{\varepsilon_o}\int ds'\, G(\vec{r},\vec{r}')\,\sigma(\vec{r}'), \qquad (8)$$

where the 2D vector $\vec{r}' = \vec{r}'(s')$ traces out the surfaces. The path of integration is along the surface, perpendicular to the local surface normal.

It is also necessary to evaluate the electric field produced by all the charges. As the electric field is the negative gradient of the potential, the field can be evaluated from Eqs.(6) and (8). For the volume sources:

$$\vec{E}(\vec{r}) = \frac{1}{\varepsilon_o}\int d^2r'\,\vec{\nabla}_r G(\vec{r},\vec{r}')\,\rho(\vec{r}'),$$
$$\vec{\nabla}_r G(\vec{r},\vec{r}') = \frac{1}{2\pi}\frac{\vec{r}-\vec{r}'}{|\vec{r}-\vec{r}'|^2}. \qquad (9)$$

For the surface charges, the result is the same, except that the volume charge density is replaced by a delta function localized at the surface. The arbitrary constant R_1 disappears from the electric field expression.

III. Overall Structure of Solution

The specification of the solution is done by means of voltage boundary conditions on conductors, typically metal surfaces. Metals are at a constant voltage,[1]

but with an unknown charge distribution at the surface. These also include highly conductive plasma interfaces. All metals will have an unknown total and surface distribution of charge, except that floating or insulated metal parts will have a fixed total charge and an unknown charge distribution and voltage. Dielectrics will have unknown surface charges to modify the fields inside the media. This takes the form of jump conditions in the normal electric field at the dielectric interface surface. Boundaries that are markers for periodic reflections of the solution will have zero normal field conditions (periodic boundary conditions).

One can see that it is necessary to break all surfaces into finite elements or increments in order to obtain an accurate numerical representation of the quantities that vary along the surfaces. Let all the elements be indexed by j, with the understanding that two materials in contact with a region of their surfaces in common will have just one set of elements in the common region. Each element will have a centroid at $\vec{r}_j$, a length ds_j, and a unit normal $\hat{n}_j$. If there is a volume charge, the volume elements, which are really incremental cross sectional areas of infinite depth in z, will be specified by the centroids $\vec{r}_j$ and the areas dA_j.

Some labels or partitionings will be introduced for the surface elements. Volume elements will be labeled by a "v" in all cases. The surface elements will be labeled with either: (1) an "m," denoting a voltage boundary condition as on a metal including floating metals, (2) an "r," denoting reflective boundary conditions with zero normal electric field, (3) a "d," denoting a dielectric interface, or (4) an "s" denoting an element in any of the surface partitions. The total number of elements in these partitions is N_v, N_m, N_r, N_d, and $N_s = N_m + N_r + N_d$.

Consider a system of voltage-specified metal surfaces with a given space charge in the volume. Together Eqs.(6) and (8) relate the voltage at the metal surface elements to the charges on the metal and in the volume. Without loss of generality, the integrals can be replaced by numerical quadratures or by sums over finite elements of the surfaces and volume to give the linear algebraic version of the system:

$$V_i^m = \sum_{j \in m} G_{i,j}^{mm} \, q_j^m + \sum_{j \in v} G_{i,j}^{mv} \, q_j^v \qquad (10)$$

$$i \in m$$

It is important to see that the only unknowns in this linear system of equations are the charge densities on the metal elements, q_j^m . All the q_j^x are defined as being the charge per length on either a surface or a volume element:

$$\begin{aligned} q_i^s &= ds_i \; \sigma(\vec{r}_i) \,, \\ q_i^v &= dA_i \; \rho(\vec{r}_i) \,. \end{aligned} \tag{11}$$

There are as many unknowns, N_m, as equations in this system described by Eq.(10). The exact procedure of discretizing Eqs.(6) and (8) will be discussed in the next sections. Eq.(10) constitutes a complete definition of the problem as formulated with potential boundary conditions and space charge. The solution of the linear system of equations for the unknown charges on each of the metal elements determines the fields everywhere in space. Note that the number of points involved in evaluating the space charge is not involved in inverting the coefficient matrix in Eq.(10). The accuracy of the solution will be determined by the number and density of elements chosen on the surfaces and volume. The numerical solutions should converge to the exact solution as the density and number of elements increase everywhere.

Now consider the next generalization, the inclusion of a reflective or periodic boundary somewhere in the system. This requires that the electric field normal to the boundary be zero and forces that boundary to be broken down into incremental elements just as if it were an actual surface. Thus there is now another set of equations numbering N_r to be added to the previous set, all derived from Eq.(9) or its surface version:

$$\begin{aligned} 0 &= \sum_{j \in m} {}^nG_{i,j}^{rm} \; q_j^m + \sum_{j \in r} {}^nG_{i,j}^{rr} \; q_j^r + \sum_{j \in v} {}^nG_{i,j}^{rv} \; q_j^v \\ &= \sum_{j \in s} {}^nG_{i,j}^{rs} \; q_j^s + \sum_{j \in v} {}^nG_{i,j}^{rv} \; q_j^v \quad . \\ i &\in r \end{aligned} \tag{12}$$

A label of "n" is used the matrix $G_{i,j}$ to denote a normal component of the gradient of the Green's function. The latter surface sum was rewritten to show that the partitions may be usefully combined.

The last illustration is the dielectric match condition. This takes the form of an inhomogeneous condition on the normal field at each element on a dielectric interface:

$$V_i^d = \sum_{j\in m} {}^nG_{i,j}^{rm}\, q_j^m + \sum_{j\in r} {}^nG_{i,j}^{rr}\, q_j^r + \sum_{j\in d} {}^nG_{i,j}^{rd}\, q_j^d + \sum_{j\in v} {}^nG_{i,j}^{rv}\, q_j^v$$
$$= \sum_{j\in s} {}^nG_{i,j}^{rs}\, q_j^s + \sum_{j\in v} {}^nG_{i,j}^{rv}\, q_j^v \quad . \qquad (13)$$
$$i \in d$$

The quantity V_i^d is of physical dimension V/m. In addition to describing the dielectric match, the d partition also contains the effects of known added amounts of charge to the faces of dielectrics. This details of this will be given later. At the moment, the purpose is to illustrate the form of the total system of equations determining the solution.

Write Eqs.(10), (12)-(13) in vector matrix notation, suppressing the indices:

$$\begin{pmatrix} \mathbf{V}^m \\ \mathbf{0} \\ \mathbf{V}^d \end{pmatrix} = \begin{pmatrix} \mathbf{G}^{ms} & \mathbf{G}^{mv} \\ {}^n\mathbf{G}^{rs} & {}^n\mathbf{G}^{rv} \\ {}^n\mathbf{G}^{ds} & {}^n\mathbf{G}^{dv} \end{pmatrix} \begin{pmatrix} \mathbf{q}^s \\ \mathbf{q}^v \end{pmatrix} . \qquad (14)$$

This can immediately be rearranged to solve for the unknown charges, $\mathbf{q}^s$:

$$\begin{pmatrix} \mathbf{G}^{ms} \\ {}^n\mathbf{G}^{rs} \\ {}^n\mathbf{G}^{ds} \end{pmatrix} \left(\mathbf{q}^s\right) = \begin{pmatrix} \mathbf{V}^m \\ \mathbf{0} \\ \mathbf{V}^d \end{pmatrix} - \begin{pmatrix} \mathbf{G}^{mv} \\ {}^n\mathbf{G}^{rv} \\ {}^n\mathbf{G}^{dv} \end{pmatrix} \left(\mathbf{q}^v\right). \qquad (15)$$

It is to be noted that the partition s contains the partitions m, r, and d, all of which are surface elements with unknown charges. Only the partition m contains known voltages. The volume charges are known, as are added dielectric surface charges which will show up in the $\mathbf{V}^d$ terms. The dimensions of the vector-matrix quantities appearing in Eqs.(14) and (15) are evident: the vectors $\mathbf{V}^x$ and $\mathbf{q}^x$ are columns of

length N_x, and matrices $\mathbf{G}^{xy}$ are N_x by N_y. The partitioned matrix on the LHS of Eq.(15) is thus square, with an equal number of unknowns and equations.

IV. Discrete Approximation of the Green's Functions

In this section the details of the formation of the linear system illustrated in Eq.(15) are given. The first item to be discussed in Section IV.A is typically the most universal of all the coupling terms. One should note that the evaluation of the potential or field at any particular surface element requires summation over all of the known and/or unknown charges in the system. Thus the coupling matrices are typically full, but also well conditioned,[3] due to the nature of the Coulomb interaction.

IV.A. Surface Potential Response to Surface Charge

Consider the potential at a surface element labeled *i* due to a surface charge distribution. The point in question is a part of the surface itself. Begin with Eq.(8) and write the integral as a sum over surface elements. Within each elemental region of the ds' integral, treat the charge as *constant*. At each point where the potential is to be evaluated, *average* the potential over the linear element. This leaves:

$$V_i \approx -\frac{1}{2\pi\varepsilon_o}\sum_j \left[\frac{1}{ds_i}\int_{ds_i} ds \frac{1}{ds_j}\int_{ds_j} ds' \ln\left(\frac{|\vec{r}-\vec{r}'|}{R_1}\right)\right] q_j \,. \qquad (16)$$

The total charge per length, $q_j = ds_j\,\sigma(\vec{r}_j)$ in C/m, has been introduced for each surface element as written in Eq.(11). Write Eq.(16) as

$$V_i^m = \sum_{j\in s} G_{i,j}^{ms}\, q_j^s \,, \qquad (17)$$
$$i \in m$$

to correspond to the vector-matrix notation introduced in Eqs.(10),(12)-(15). Since the potential is only needed at the metal (m) elements, the range of i is restricted to the m partition. Note that $G_{i,j}$ is not the same physical dimension as the dimensionless 2D Green's function G in Eq.(5), as the $-1/\varepsilon_o$ constant in the PE is now included.

For $i \neq j$ the sum-and-average integrals of the Green's function over the finite element can be approximated as

$$G_{i,j}^{ms} \approx -\frac{1}{2\pi\varepsilon_o} \ln\left(\frac{\left|\vec{r}_i - \vec{r}_j\right|}{R_1}\right), \qquad (18)$$
$$i \in m, j \in s, i \neq j \ .$$

This is valid if the surface is smooth, meaning that, approximately, $\left|\vec{r}_i - \vec{r}_j\right| \geq ds_i$ or ds_j. A surface with sharp bends may need refinement of the incrementation. For $i = j$, the diagonal term in Eq.(16) requires a more precise evaluation because of the self-interaction singularity. The diagonal coupling term can be reduced (with some algebra) to

$$G_{i,i}^{ms} = -\frac{1}{2\pi\varepsilon_o}\left(\ln\left(\frac{ds_i}{R_1}\right) - \frac{3}{2}\right). \qquad (19)$$

In the case of a collinear line of equal-length surface elements, the largest relative errors introduced by approximating Eq.(16) by Eq.(18) are 10% for nearest neighbors and 2% for next-nearest neighbors, as derived by analysis of the sum-and-average integrals in Eq.(16). Although it is possible to improve the accuracy by use of coupling terms which depend on the orientation of the individual elements, it does not seem worthwhile, since a systematic reduction in error can be achieved by increasing the number and density of the finite elements.

IV.B. Surface Potential Response to Volume Charge

If there is a space charge in the system, the potential of that charge must be computed from Eq.(6) just as indicated in Eqs.(10) and (15). This involves no self-interaction terms in order to evaluate the potential on the metal surfaces, so the result can be approximated as previously done for the non-diagonal surface-surface terms:

$$V_i^m \approx \sum_{j \in v} G_{i,j}^{mv}\, q_j^v\,,$$

$$i \in m$$

$$G_{i,j}^{mv} = -\frac{1}{2\pi\varepsilon_o}\frac{1}{ds_i}\int_{ds_i} ds \frac{1}{dA_j}\int_{dA_j} d^2r'\,\ln\left(\frac{|\vec{r}-\vec{r}'|}{R_1}\right), \qquad (20)$$

$$\approx -\frac{1}{2\pi\varepsilon_o}\ln\left(\frac{|\vec{r}_i-\vec{r}_j|}{R_1}\right).$$

Any improvement in this result would involve incorporating information about the shape of the volume elements next to the surface. As it stands, one might refer to the result in Eq.(20) as a "wire-wire" interaction appropriate for the far-field of the interaction between the finite elements.

IV.C. Imposition of Reflective Boundary Conditions

Reflective boundary conditions, which are used to restrict the solution region to a small part of the total space of the problem, generate periodic replicas of the solution as one moves across the boundary. Of course what is really imposed is the vanishing of the electric field component normal to the surface zone in question. Unless the conditions are logically set up and consistent, the reflective boundary condition will only generate a perplexing field solution which has surface elements with unusual field conditions imposed. With this caution in place, the analysis proceeds as follows.

Consider the field at a boundary point in the "r" partition due to all charges in the system, both on surface and in volume, as given by Eq.(9):

$$\vec{E}(\vec{r}) = \frac{1}{\varepsilon_o}\int ds'\,\vec{\nabla}_r G(\vec{r},\vec{r}')\,\sigma(\vec{r}') + \frac{1}{\varepsilon_o}\int d^2r'\,\vec{\nabla}_r G(\vec{r},\vec{r}')\,\rho(\vec{r}')\,. \qquad (21)$$

The gradient of the Green's function is given in Eq.(9). Choose $\vec{r}$ to be arbitrarily close to the surface of point i, and dot the field with the unit normal of element i to find the component of field normal to that surface element. The result should be zero:

$$\hat{n}_i \cdot \vec{E}(\vec{r}_i) = 0 = \frac{1}{\varepsilon_o}\int ds'\, \hat{n}_i \cdot \vec{\nabla}_r G(\vec{r},\vec{r}\,')\sigma(\vec{r}\,') + \frac{1}{\varepsilon_o}\int d^2r'\, \hat{n}_i \cdot \vec{\nabla}_r G(\vec{r},\vec{r}\,')\rho(\vec{r}\,') . \tag{22}$$

Approximate the integrals in Eq.(22) as sums of terms assuming that the charges are *constant* within each of the surface and volume intervals, as before. This allows the introduction of the charge per length quantities, q_j^s and q_j^v . The result is precisely as symbolized in Eq.(12) with:

$$ {}^nG_{i,j}^{rs} = \frac{1}{\varepsilon_o}\frac{1}{ds_j}\int_{ds_j} ds'\, \hat{n}_i \cdot \vec{\nabla}_r G(\vec{r}_i,\vec{r}\,') \approx \frac{1}{2\pi\varepsilon_o}\frac{\hat{n}_i \cdot (\vec{r}_i - \vec{r}_j)}{\left|\vec{r}_i - \vec{r}_j\right|^2} \tag{23}$$

$$i \neq j, \quad i \in r, \quad j \in s$$

and

$$ {}^nG_{i,j}^{rv} = \frac{1}{\varepsilon_o}\frac{1}{dA_j}\int_{dA_j} d^2r'\, \hat{n}_i \cdot \vec{\nabla}_r G(\vec{r}_i,\vec{r}\,') \approx \frac{1}{2\pi\varepsilon_o}\frac{\hat{n}_i \cdot (\vec{r}_i - \vec{r}_j)}{\left|\vec{r}_i - \vec{r}_j\right|^2} . \tag{24}$$

$$i \in r, j \in v$$

The volume sources are not concerned with self-interaction, but the surface-surface relation in Eq.(23) must be evaluated for that case. The integral is truly discontinuous as $\vec{r}$ is carried through the plane of the element. The analytic evaluation of the self-interaction term gives:

$$ {}^nG_{i,i}^{rr} = \frac{1}{2\pi\varepsilon_o}\frac{1}{ds_i}\int_{ds_i} ds'\, \frac{\hat{n}_i \cdot (\vec{r}_i - \vec{r}\,')}{\left|\vec{r}_i - \vec{r}\,'\right|^2} = \pm\frac{1}{2\pi\varepsilon_o}\frac{\pi}{ds_i} \tag{25}$$

with the positive sign when the unit normal points toward the "computational side" of the element. This is the same as knowing that the electric field about a sheet of positive charge points away from the sheet on both sides and has the magnitude $\sigma / 2\varepsilon_o$ on each side.[1,2] The averaging that was done previously in order to obtain an improved self-interaction term is not necessary here as the limiting values in Eq.(25)

are obtained anywhere along the finite surface element. The $\pm$ sign in Eq.(25) will be fixed at + by setting up the unit normal vectors such that they point towards the computational side of the periodic boundary.

Eqs.(23)-(25) fill in the definitions of the $\mathbf{G}^{rx}$ partitions of the matrices as they appear in Eq.(14) or (15). A detail is the specification and storage of the unit normal vectors. Specifically arrays of the sin and cos of the unit normals are stored at the solution outset and used in the evaluation of the dot products when needed.

IV.D. Imposition of Dielectric Matching Conditions

These conditions are slightly more complex than the reflective boundary condition case in the last subsection, but they are not the most subtle - that is saved for last! The treatment of dielectrics provided here for the purposes of field calculation is that they are replaced with charged boundary layers at their actual surfaces.[1] These charged layers serve to modify the applied fields in order to obtain the correct field strength within the dielectric medium. It is true that there are fundamental reasons why the presence of dielectrics can be analyzed as a vacuum problem with inserted bodies of matter.[1,4] Since the problems being addressed here are in electrostatics with homogeneous and isotropic media throughout, the formulation is particularly simple. Of course the *whole* problem is not homogeneous and isotropic. All dielectric media will be free of internal charge. The only distributed charge density occurs in the vacuum regions which can contain plasma space charge. The dielectric surfaces, whether between two dielectrics in contact or between a dielectric and the vacuum, will have an unknown amount of surface charge that is sufficient to produce the normal electric field discontinuity required by the macroscopic descriptions. In addition, a prescribed amount of deposited surface charge may be added to represent such charging of dielectric media in contact with a plasma.

Consider, without loss of generality, the following 1D problem in coordinate x. On the right side of the boundary, say for $x > 0$, there is material 1 with permittivity (dielectric constant) ε_1 ; on the left, for $x < 0$ there is material 2 with permittivity ε_2. Let the (x-component) electric field for $x \to 0^-$ be $E_<$ and the field for $x \to 0^+$ be $E_>$. The fields are space dependent, so the values near the boundary are to be used. First consider the case with no added surface charge; the dielectric match condition is[1]

$$\varepsilon_2 E_< = \varepsilon_1 E_> . \tag{26}$$

A "polarization charge" σ^{pol} will be added to the surface to reproduce the jump. Let the field near the boundary be the sum of the fields due to all other sources evaluated at that point, say, E^{other}, and the field due to σ^{pol}. E^{other} must be *continuous* across the boundary. Substituting into Eq.(26) gives:

$$\begin{aligned} \varepsilon_2 E_< &= \varepsilon_2 \left(E^{other} - \frac{\sigma^{pol}}{2\varepsilon_o} \right) \\ &= \varepsilon_1 E_> = \varepsilon_1 \left(E^{other} + \frac{\sigma^{pol}}{2\varepsilon_o} \right) \end{aligned} \tag{27}$$

from which one solves for σ^{pol}:

$$\sigma^{pol} = \frac{\varepsilon_2 - \varepsilon_1}{\varepsilon_2 + \varepsilon_1} 2\varepsilon_o E^{other} . \tag{28}$$

Now write down the expression for the normal component of the electric field at the above boundary, say element i, due to all other charges in the system:

$$E^{other} = \hat{n}_i \cdot \vec{E}(\vec{r}_i) = \sum_{\substack{j \in s \\ j \neq i}} {}^{n}G_{i,j}^{ds} \, q_j^s + \sum_{j \in v} {}^{n}G_{i,j}^{dv} \, q_j^v . \tag{29}$$

In order for the sign of Eq.(29) to be correct, the unit normal must point towards positive x, in other words, from medium with ε_2 to medium with ε_1. The ${}^{n}G_{i,j}^{xy}$ matrices are defined in Eqs.(23)-(25). Combining Eqs.(28) and (29) and replacing $\sigma^{pol} = q_i^d \, / \, ds_i$ gives

$$0 = \frac{1}{2\pi\varepsilon_o} \frac{\pi}{ds_i} \frac{\varepsilon_1 + \varepsilon_2}{\varepsilon_1 - \varepsilon_2} q_i^d + \sum_{\substack{j \in s \\ j \neq i}} {}^{n}G_{i,j}^{ds} \, q_j^s + \sum_{j \in v} {}^{n}G_{i,j}^{dv} \, q_j^v , \tag{30}$$

$$i \in d$$

which is a homogeneous equation in the surface charges similar to the reflective boundary condition partition defined in Section IV.C. A convenient way of expressing Eq.(30) is to define the diagonal of the coupling matrix as:

$$ {}^{n}G^{dd}_{i,i} = \frac{1}{2\pi\varepsilon_o}\,\frac{\pi}{ds_i}\,\frac{\varepsilon_1+\varepsilon_2}{\varepsilon_1-\varepsilon_2}\ . \qquad i\in d \tag{31} $$

The limit of $\varepsilon_2 \to \varepsilon_1$ gives a diagonal non-singular system in Eq.(30) and forces all $q_i^d \to 0$, as it should. This completes the dielectric match, except for the inclusion of added surface charge.

Let a deposited surface charge, $\sigma^{add} = q^{add} / ds_i$, be present on the boundary element. This added charge can be displaced away from the boundary surface by a infinitesimal amount and the previous solution for a dielectric match of an uncharged surface can be used again. The displacement must be *towards* the vacuum side of the interface to be consistent with a plasma charge deposition mechanism. In the 1D model above this displacement is characterized by a $\pm$. Thus if the top sign is chosen, dielectric medium 1 is vacuum and $\varepsilon_1 = \varepsilon_o$; if the bottom sign, $\varepsilon_2 = \varepsilon_o$. The field symbolized by E^{other} is now the field due to the charges on all other surface and volume elements, *plus* the field due to the infinitesimally-displaced added charge layer, namely $\mp\sigma^{add} / 2\varepsilon_o$. The charge on the surface element in question is the sum of the polarization and added charges:

$$ q^{pol} + q^{add} = q_i^d\ . \tag{32} $$

After eliminating q^{pol} and using the permittivities to remove the $\pm$ sign, one obtains Eq.(30) with an inhomogeneous term:

$$ \frac{1}{\varepsilon_1-\varepsilon_2}\,\frac{q_i^{add}}{ds_i} = \frac{1}{2\pi\varepsilon_o}\,\frac{\pi}{ds_i}\,\frac{\varepsilon_1+\varepsilon_2}{\varepsilon_1-\varepsilon_2} q_i^d + \sum_{\substack{j\in s\\ j\neq i}} {}^{n}G^{ds}_{i,j}\, q_j^s + \sum_{j\in v} {}^{n}G^{dv}_{i,j}\, q_j^v \qquad i\in d \tag{33} $$

Of course the diagonal term on the RHS can be defined into the coupling matrices. The LHS of Eq.(33) is the i'th element of the column vector called V^d in Eqs.(14) and (15).

This completes the construction of the linear algebraic equivalent of the integral equation to be solved for the surface charges. Still to do is the case alluded to as the most subtle of the tasks.

IV.E Insulated (Floating) Conducting Bodies

In the study of plasma interaction with surfaces, part of the conducting material in contact with the plasma can be with prescribed voltage and unknown charge, as dealt with earlier in Section IV.A. However a conductor that is electrically insulated will have a known (or determinable) total charge and an unknown voltage and charge distribution on its surface. This would seem to be a formidable problem in potential theory, but the numerical resolution in the context of the surface Green's function methods is quite simple once unveiled.

Rewrite Eq.(15) as

$$\sum_j A_{i,j}\, x_j = b_i \tag{34}$$

where $\mathbf{A}$ denotes the square matrix of $\mathbf{G}^{xs}$ coefficients, $\mathbf{x}$ denotes the unknown surface charge vector $\mathbf{q}^s$, and $\mathbf{b}$ the whole RHS vector. Let each insulated conducting body be a subset of the "m" partition in the problem. Give each body a unique label say "k". Let the total charge per length on body k be Q_k. The incorporation of this information into the solution proceeds as follows:

(i) Calculate all of the elements in $\mathbf{A}$ and $\mathbf{b}$ as if the insulated bodies are of specified voltage boundary conditions, as usual in the m partition.

(ii) Search through the rows of $\mathbf{A}$ to find the first member of subpartition k. Say this happens to be row i.

(iii) Find the next member of subpartition k. Say that this is row n.

(iv) Replace row i in A and b with

$$A_{i,j} \rightarrow A_{i,j} - A_{n,j}\,, \quad b_i \rightarrow 0$$
$$\text{for all } j$$

This relation incorporates the condition that the voltage difference between row i and row n (surface elements i and n) is zero, as must be true for a conductor. Remove row i from examination.

(v) Redo the search for members of k, treating row n as the new row i. Repeat (iii) through (v) as long as members of k are found.

(vi) If there is not another member of subpartition k, then replace row i in $\mathbf{A}$ and $\mathbf{b}$ with:

$$A_{i,j} = 1, \quad j \in k,$$
$$A_{i,j} = 0, \quad j \notin k,$$
$$b_i = Q_k ,$$

insuring specification of total charge on the subpartition k.

The above must be repeated for all insulated bodies (all distinct k) in the system. One proceeds to solve this transformed $\mathbf{A}$ and $\mathbf{b}$ to generate the charges on all the surface elements. Note that no change in dimension or redoing of the interaction matrix element was necessary to carry out the insulated conductor modification.

V. Evaluation of the Fields from the Charges

The solution of the linear system of equations presented by Eq.(15) is done by a full-pivoting Gauss-Jordan elimination code given in "Numerical Recipes"[3]. No problems with the numerical conditioning have been found for any well-formulated problem with up to 700 surface elements using 64-bit arithmetic. The computational time is slower with the larger dimensions, of course.

Finding the potential and electric fields is a straightforward procedure based on evaluation of the integrals in Eqs.(6), (8), and (21) once the surface charges are found. At first the fields were evaluated by the same algorithms as presented in Section IV. However it became obvious that the evaluation procedure was not as smooth as expected near boundary surfaces. One cause of this is that the evaluation "grid" or sample space is not directly connected to the finite element setup for the surfaces or the volume charge, if there is one. Thus one may evaluate the fields very close to the surfaces, on the surfaces, or wherever. This difficulty was remedied by using the exact field of a 2D finite element with uniform charge as the source term for all the

charged surface elements. The more approximate treatment is just a modified far-field approximation to this procedure.

The general 2D expression for the potential field due to a collection of surface and volume charges each with a uniform distribution of charge is

$$V(\vec{r}) = -\frac{1}{2\pi\varepsilon_o}\sum_{j\in s}\left[\frac{1}{ds_j}\int_{ds_j} ds'\,\ln\left(\frac{|\vec{r}-\vec{r}\,'(s')|}{R_1}\right)\right]q_j \\ -\frac{1}{2\pi\varepsilon_o}\sum_{j\in v}\left[\frac{1}{dA_j}\int_{dA_j} d^2r'\,\ln\left(\frac{|\vec{r}-\vec{r}\,'|}{R_1}\right)\right]q_j\,. \tag{35}$$

The electric field could be evaluated by two schemes: either compute the potential field and take numerical finite differences to get the electric field, or evaluate the electric field directly from the charge sources as symbolized in Eq.(21). Some applications may prefer the first approach because of its flexibility, but here the second is emphasized because of its speed and efficiency. The general expression for the electric field is the negative of the gradient of Eq.(35):

$$\vec{E}(\vec{r}) = \frac{1}{2\pi\varepsilon_o}\sum_{j\in s}\left[\frac{1}{ds_j}\int_{ds_j} ds'\,\frac{\vec{r}-\vec{r}\,'(s')}{|\vec{r}-\vec{r}\,'(s')|^2}\right]q_j \\ +\frac{1}{2\pi\varepsilon_o}\sum_{j\in v}\left[\frac{1}{dA_j}\int_{dA_j} d^2r'\,\frac{\vec{r}-\vec{r}\,'}{|\vec{r}-\vec{r}\,'|^2}\right]q_j\,. \tag{36}$$

All the q_j in the above are known. If one can analytically evaluate the integrals in Eq.(35) and (36), the fields are just a summation away from done. The integrals, where doable, are difficult, and secondly the unknown shape of the volume decomposition prevents an exact expression for those terms.

V.A. Fields from the Charges - More Approximate Method

Consider the potential evaluation first. If $\vec{r}$ and $\vec{r}\,'$ are sufficiently separate, the quantities in brackets in Eq.(35) may be simplified by a far-field approximation

exactly as done in Eqs.(18) and (20). If $\vec{r}$ is within the near-zone of surface element j, the averaged value given in Eq.(19) can be used. An analogous average procedure for the volume when $\vec{r}$ is near volume element j gives

$$-\frac{1}{2\pi\varepsilon_o}\left(\ln\left(\frac{r_x}{R_1}\right)-\frac{1}{4}\right), \qquad (37)$$
$$\pi r_x^2 = dA_j ,$$

for the coefficient of q_j. This assumes that the cross sections dA_j are *circular* in order to be able to analytically evaluate the constant term in Eq.(37). The above is not useful unless the far-field formulae and near-field averages can be joined. Actually they combine fairly well by switching between the two limiting forms at the separation where the terms are equal.

The electric field analog of this approximation of the potential is not so encouraging. The far-field approximations are fine, but the near-field averages as presented in Eqs.(19) and (37) give a constant or zero electric field contribution of the nearby charge density to the total field at that point. This is not grossly in error, but the numerical effect is to produce an "interference" rippling of the evaluated (total) fields when the spacing of the evaluation grid was not identical to the spacing in the volume grid used to input the space charge. Also the fields tended to ripple when evaluated in the near-field zone of the surface elements. The relative errors typically were not large, but the appearance was convincing enough to prompt for a direct evaluation of the integrals in Eqs.(35) and (36).

V.B. Fields from the Charges - Analytic Surface Elements

The fields about a uniformly charged strip can be evaluated exactly.[2] Thus the surface integrals in Eq.(35) can be expressed in terms of elementary functions. As mentioned previously though, the volume elements are of unspecified shape and thus not so amenable. The surface treatment is given now.

Consider term j, $j \in s$, in Eq.(35). Recall that the surface elements have a length ds_j, centroid $\vec{r}_j$, and a unit normal $\hat{n}_j$. Set up a rotated x-y coordinate system with positive y along the unit normal and the origin at the centroid of the element. This allows the 1D integration to be expressed precisely:

$$
\begin{aligned}
&-\frac{1}{2\pi\varepsilon_o} q_j \frac{1}{ds_j} \int_{ds_j} ds' \ln\left(\frac{|\vec{r}-\vec{r}\,'(s')|}{R_1}\right) \\
&\quad = -\frac{1}{4\pi\varepsilon_o} q_j \frac{1}{ds_j} \int_{-ds_j/2}^{ds_j/2} dx' \ln\left(\frac{(x'-x)^2+y^2}{R_1^2}\right) \\
&= -\frac{1}{4\pi\varepsilon_o} q_j \int_{-1/2}^{1/2} dx' \left(\ln\left(ds_j^2 / R_1^2\right) + \ln\left((x'-x)^2+y^2\right)\right) \\
&\quad = -\frac{1}{4\pi\varepsilon_o} q_j \left(2\ln\left(\frac{ds_j}{R_1}\right) + \int_{-1/2-x}^{1/2-x} dt \ln\left(t^2+y^2\right)\right).
\end{aligned}
\tag{38}
$$

The latter form was obtained by scaling all the coordinates with the element length and shifting the integration variable. Use of the indefinite integral,

$$
\int dx \ln(x^2+a^2) = x\ln(x^2+a^2) - 2x + 2a\arctan(x/a) \tag{39}
$$

allows the result to be computed, with the rotation and scaling still present:

$$
\begin{aligned}
-\frac{1}{2\pi\varepsilon_o} q_j \frac{1}{ds_j} \int_{ds_j} ds' \ln\left(\frac{|\vec{r}-\vec{r}\,'(s')|}{R_1}\right) &= -\frac{1}{2\pi\varepsilon_o} q_j \left[\ln\left(\frac{ds_j}{R_1}\right) - 1\right. \\
&+ y\arctan\left(\frac{1-2x}{2y}\right) + y\arctan\left(\frac{1+2x}{2y}\right) \\
&+ \frac{1-2x}{4}\ln\left((1/2-x)^2+y^2\right) \\
&\left. + \frac{1+2x}{4}\ln\left((1/2+x)^2+y^2\right)\right].
\end{aligned}
\tag{40}
$$

An analogous integration for the electric field term from Eq.(36) gives:

$$\frac{1}{2\pi\varepsilon_o} q_j \frac{1}{ds_j} \int_{ds_j} ds' \frac{\vec{r} - \vec{r}\,'(s')}{|\vec{r} - \vec{r}\,'(s')|^2} =$$

$$\frac{1}{2\pi\varepsilon_o} q_j \frac{1}{ds_j} \left[\frac{1}{2} \hat{e}_x \ln\left(\frac{(x+1/2)^2 + y^2}{(x-1/2)^2 + y^2} \right) \right. \tag{41}$$

$$\left. + \hat{e}_y \left(\arctan\left(\frac{1/2 - x}{y} \right) + \arctan\left(\frac{1/2 + x}{y} \right) \right) \right].$$

These formulae are used for the surface evaluations, admittedly with the added complexity of accounting for the orientation of the surface elements.

V.C. Fields from the Charges - Analytic Volume Elements

The potential and field about a space charge element in the volume are difficult to evaluate because of the arbitrary shape. If the volume elements are modeled as being infinite cylinders of circular cross section, the fields can be found exactly. Consider term j, $j \in v$, in the general expression for the potential field given by Eq.(35):

$$-\frac{1}{2\pi\varepsilon_o} q_j \frac{1}{dA_j} \int_{dA_j} d^2 r' \ln\left(\frac{|\vec{r} - \vec{r}\,'|}{R_1} \right)$$

$$= -\frac{1}{2\pi\varepsilon_o} q_j \begin{cases} \ln\left(\dfrac{R}{R_1} \right) & , \; R > r_x \\ \ln\left(\dfrac{r_x}{R_1} \right) - \dfrac{1}{2} + \dfrac{R^2}{2 r_x^2} & , \; R < r_x \end{cases} \tag{42}$$

where $R = |\vec{r} - \vec{r}_j|$ is the distance of $\vec{r}$ from the center $\vec{r}_j$ of the element of area $dA_j = \pi r_x^2$. Eq.(42) can be differentiated to give the analogous term in the expression for the electric field in Eq.(36):

$$\frac{1}{2\pi\varepsilon_o} q_j \frac{1}{dA_j} \int_{dA_j} d^2r' \frac{\vec{r}-\vec{r}'}{|\vec{r}-\vec{r}'|^2}$$
$$= \frac{1}{2\pi\varepsilon_o} q_j \hat{e}_R \begin{cases} 1/R & , R>r_x \\ R/r_x^2 & , R<r_x \end{cases} \tag{43}$$

where $\hat{e}_R$ is the radial unit vector pointing from $\vec{r}_j$ to $\vec{r}$.

The volume average of the potential term in Eq.(42) can be done over the elemental area as a check -- the result agrees with Eq.(37).

VI. Example Solutions and Discussion

There are an innumerable number of illustrations and examples that can be given to illustrate the Poisson solver. A few are given here which are representative of the many tests that have been carried out.

The first is a series of computations for the potential around two charged strips as the number of finite elements is varied on the strips. Only the potential is shown here. Fig. 1 shows a "wire mesh plot" of the potential for a strip separation of 0.5m, a strip width of 1.0m, a plotting field of 2m on a side with 50 points in each direction, a voltage of +1V on the upper strip, a voltage of -1V on the lower strip, and *one* finite element on each strip. The rounded nature of the potential as one moves across the strips is due to the structure of the formula in Eq.(40). One recalls that a metal strip of constant voltage does not really have a constant charge distribution as assumed in this "one element model." The correct distribution of charge is found by including several elements within each strip and thus allowing the potential at the strip to become constant. In Fig.2 the number of divisions on each strip is raised to 5. In Fig. 3 it is 10, and in Fig. 4 it is 50. In fact the results are converged at 50 as seen in calculations (not shown) with 100 and 500 points in each strip.

The effect of reflective boundary conditions is shown in Figs. 5 and 6 for the case of two parallel wires separated by 0.5m and charged to +1V and -1V. Reflective boundary conditions were imposed at x=1m and -1m with 100 intervals along each boundary.

A space charge solution is shown in Figs. 7 through 10. The potential of a rod with a Gaussian distribution of charge is evaluated within a 2m by 2m box. The characteristic radius of the charge is 0.25m and the evaluation grid is 50 by 50. The absolute scale of the potential is arbitrary because of the boundary conditions. Fig. 7

shows the potential over the evaluation volume and Fig. 8 shows the y-component of the electric field, E_y. In Fig. 9 the potential is evaluated on a 50 by 50 grid in the *center* of the full scale region. The scale has been magnified by a factor of 10; thus the fields are being evaluated throughout the finite volume elements used for the construction of the solution. The same is shown for E_y in Fig. 10 and to be noticed is the oscillation which is due to the replacement of the actual square volume elements by the circular approximation as discussed in Section V.C. The ripples are present in Fig.9, but are much less noticeable because of the actually small relative error present in Fig. 10. Figs. 7-10 show the most obvious error present in the Green's function method for solving the Poisson equation as it is formulated here. The practical rule to avoid the ripple shown in Fig. 10 is to simply evaluate the potential and/or the electric field on the same grid in the volume as used for the representation of the charge density, with intermediate values obtained by interpolation. Fig. 8 shows that this procedure gives smooth and eye-pleasing results.

The last example shows a feature similar to that in the surface topography of microelectronic processing. The computation volume is a $10\,\mu$m by $10\,\mu$m section with a $1\,\mu$m silicon oxide layer laid on the bottom surface. There is a $3\,\mu$m high by $4\,\mu$m wide feature of polysilicon in the center which is covered with a $1\,\mu$m thick layer of oxide. The oxide is an insulator and subject to plasma-produced charging. The polysilicon is a good conductor and is thus at equipotential. The surfaces are all decomposed into element of length $0.1\,\mu$m and the evaluation grid for construction of the surface plots is a 100 by 100 grid with spacing of $0.1\,\mu$m. The voltage of the top (plasma) surface is held at 0V and the bottom is held at -5V. In Fig. 11 the collected charge on the polysilicon feature is left at zero. The dielectric regions are visible as "depressions" in the potential field. The polysilicon is the rectangular region of constant potential. In Fig. 12 the charge on the polysilicon is allowed to increase, which raises the potential and the surrounding fields. In Fig. 13 a positive surface charge is placed on the bottom dielectric layer and a negative surface charge on the top of the oxide layer on top of the polysilicon. These are presented to illustrate the capabilities of the solution method, not any particular microelectronic situation.

Any or all of the features of the PE solution discussed in these examples can be combined in a single problem, including the presence of more than one floating conducting bodies.

Appendix

There is one complication in using any PE solver with a space charge that must be discussed. Consider a parallel plate system with a space charge ρ between the plates, separated by L. This space charge will almost always be the difference between a positive ion density and an electron density -- a plasma in other words. Suppose for the moment that the positive and negative charge densities are equal; thus there is no macroscopic charge and ρ is zero. Now solve the PE with a potential difference ΔV imposed on the plates. The field is just $E = -\Delta V / L$, constant between the plates. Now consider the dynamical solution for the response of the particles to this field. The electrons will respond quickly, on a time scale of the electron plasma frequency,[5]

$$\omega_{pe} = \sqrt{n_e e^2 / \varepsilon_o m_e} \qquad \text{(A1)}$$

which, if the plasma density is high, creates an extremely fast motion which must be resolved with a small time incrementation. Standard notation is used for the symbols in this Appendix. The system will eventually converge to a slowly evolving (quasi-steady-state) solution in which the bulk of the plasma has a very small electric field, with the presence of plasma charge separations near the plates (sheaths) which cancel out the bulk electric field. The thickness of the regions of charge separation is the Debye length,[5]

$$\lambda_D = \sqrt{\varepsilon_o kT_e / e^2 n_e}\,, \qquad \text{(A2)}$$

which can be very small compared to the size of the bulk plasma region. In bulk high density plasmas, the electron mobility and diffusion may be shown to drive the electric field to an asymptotic value (ambipolar field),

$$\vec{E} \approx -\frac{kT_e}{e}\frac{\vec{\nabla} n_e}{n_e}. \qquad \text{(A3)}$$

This is a well known effect and numerical methods exist to help stabilize the solution.[6,7]

Acknowledgments

I wish to thank Bob Campbell for several useful discussions regarding this work. This work was supported by the U. S. Department of Energy under Contract DE-AC04-94AL85000. Sandia is a multiprogram laboratory operated by Sandia Corporation, a Lockheed Martin Company, for the United States Department of Energy.

References:

1. Leonard Eyges, "The Classical Electromagnetic Field," Dover Publications, Inc., New York, NY, 1980.

2. P. M.. Morse and H. Feshbach, "Methods of Theoretical Physics," Chs. 7, 10, and 11, McGraw-Hill Book Co., New York, NY, 1953.

3. W. H. Press, B. P. Flannery, S. A. Teukolsky, and W. T. Vetterling, "Numerical Recipes," Cambridge Univ. Press, New York, NY, 1986.

4. R. P. Feynman, R. B. Leighton, and M. Sands, "The Feynman Lectures on Physics," Vol. II, Ch. 10, Addison-Wesley Pub. Co. Reading, MA, 1989 issue.

5. D. C. Montgomery and D. A. Tidman, "Plasma Kinetic Theory," McGraw-Hill Book Co., New York, NY, 1964.

6. P. L. G. Ventzek, R. J. Hoekstra, M. J. Kushner, "2-Dimensional Modeling of High Plasma Density Inductively Coupled Sources for Materials Processing", J. Vac. Sci. Tech. B. 12, 461 (1994).

7. M. J. Kushner, W. Z. Collison, M. J. Grapperhaus, J. P. Holland and M. S. Barnes, "A 3-dimensional Model for Inductively Coupled Plasma Etching Reactors: Azimuthal Symmetry and Coil Properties", J. Appl. Phys. 80, 1337 (1996).

Figure 1. This is a "wire mesh plot" of the potential between two parallel charged strips separated by 0.5m where each strip has a width of 1.0m. The potential boundary condition is +1V on the upper strip and -1V on the lower strip The plotting field is 2m on a side with 50 points in each of the x and y directions. The important point here is that there is just *one* finite element on each strip. The variation of the potential as one moves across the strips is due to the limited resolution of the single finite element. A metal strip of constant voltage does not have a constant charge distribution as assumed in the evaluation of the field about a single element.

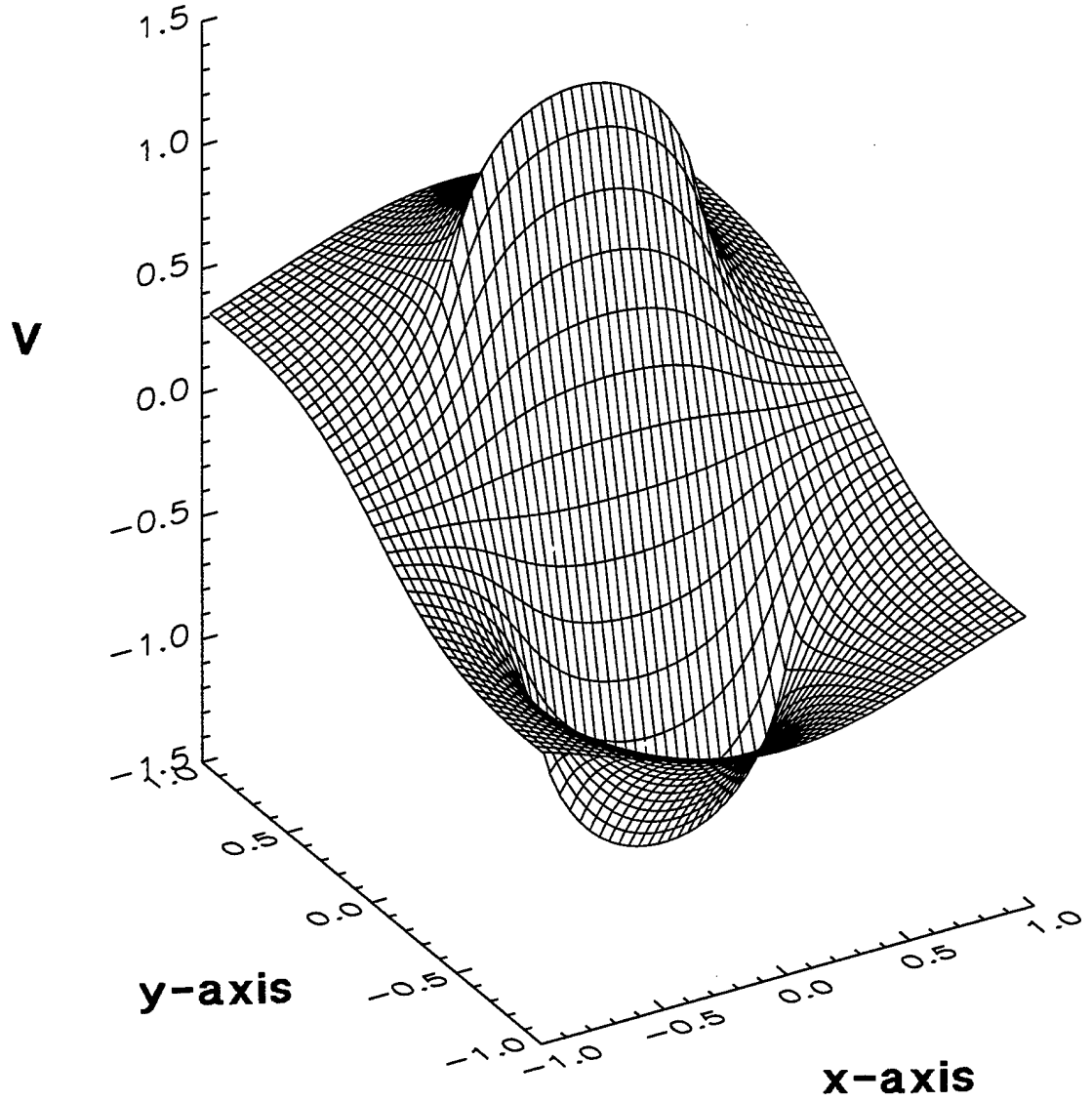

Fig.1

Figure 2. Same as Fig.1 except in the resolution of the charged strips. Here there are *five* finite elements on each strip. The potential at each strip is now more constant in accord with the imposed boundary conditions.

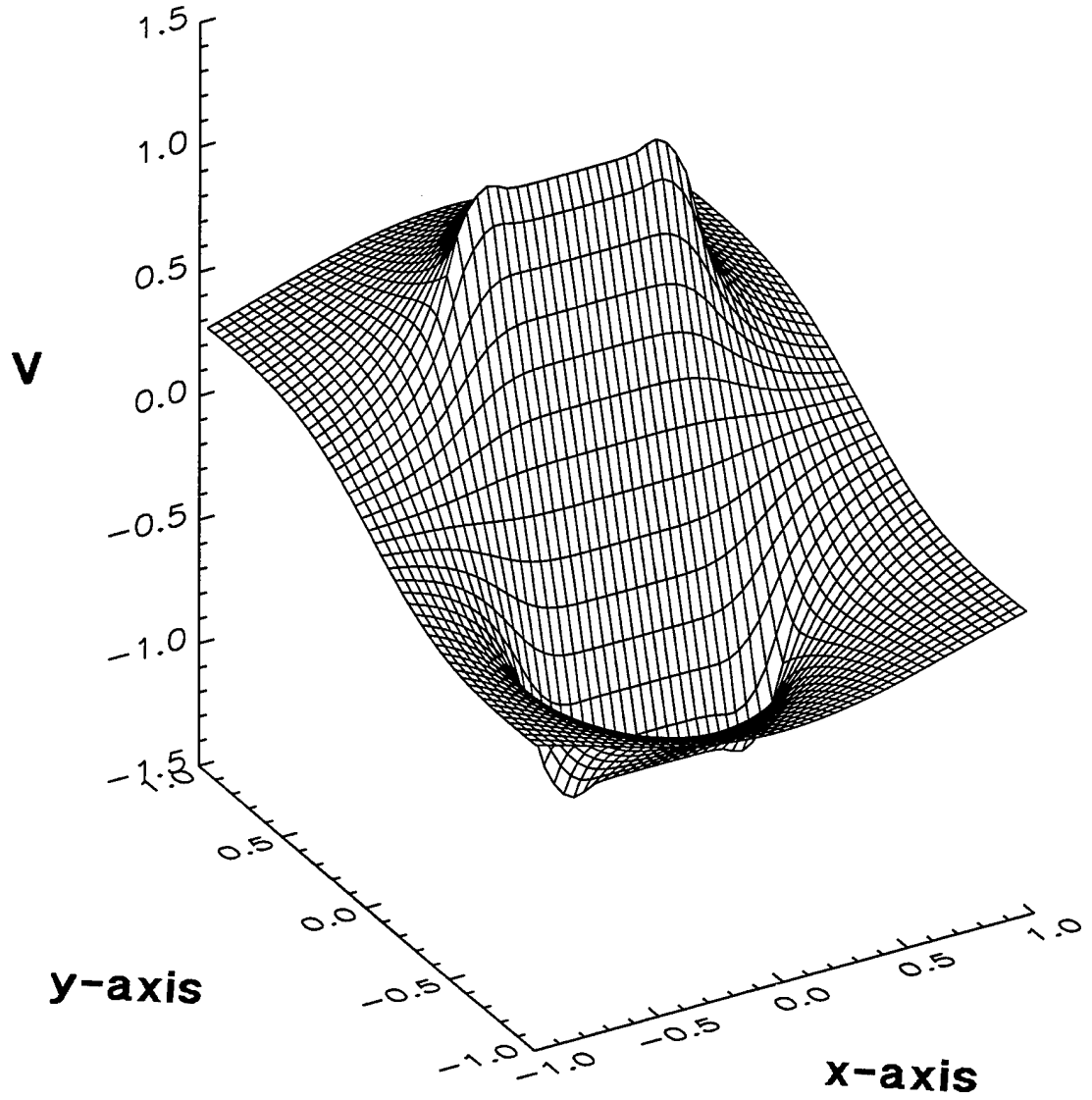

Fig.2

Figure 3. Same as Figs.1 and 2 except in the resolution of the charged strips. Here there are *ten* finite elements on each strip. The potential at each strip is even more constant in accord with the imposed boundary conditions.

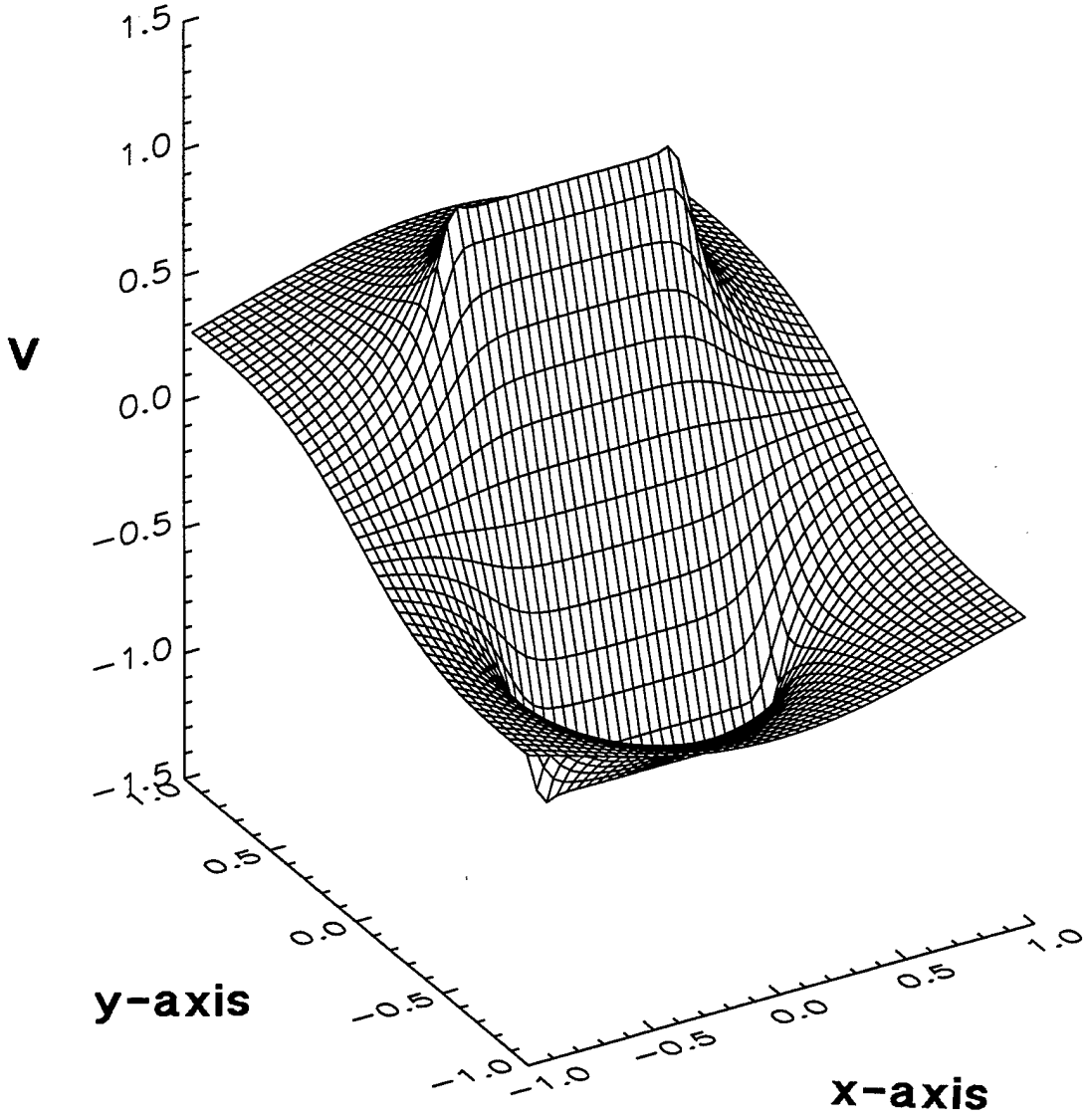

Fig.3

Figure 4. Same as Figs.1, 2, and 3, except in the resolution of the charged strips. Here there are *fifty* finite elements on each strip. The potential at each strip has converged as demonstrated by calculations using 100 and 500 elements per strip (not shown) which appear identical to this result.

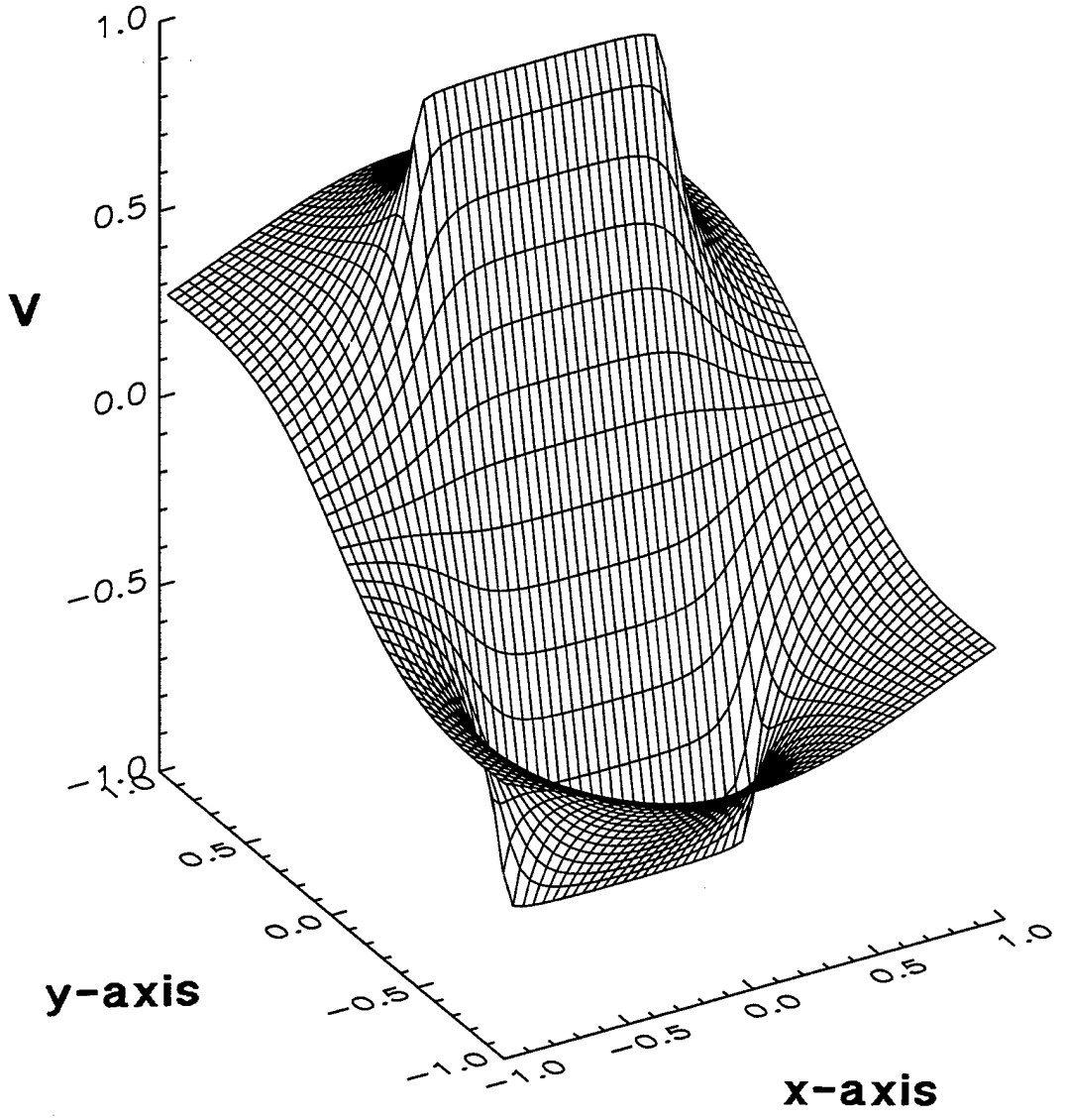

Fig.4

Figure 5. A contour plot of the potential for the case of two parallel wires (really short surface elements) separated by 0.5m and charged to +1V and -1V. No boundary conditions were imposed on the sides so that free space conditions are seen within the computational volume. The contours near the charged wires are suppressed for presentation clarity.

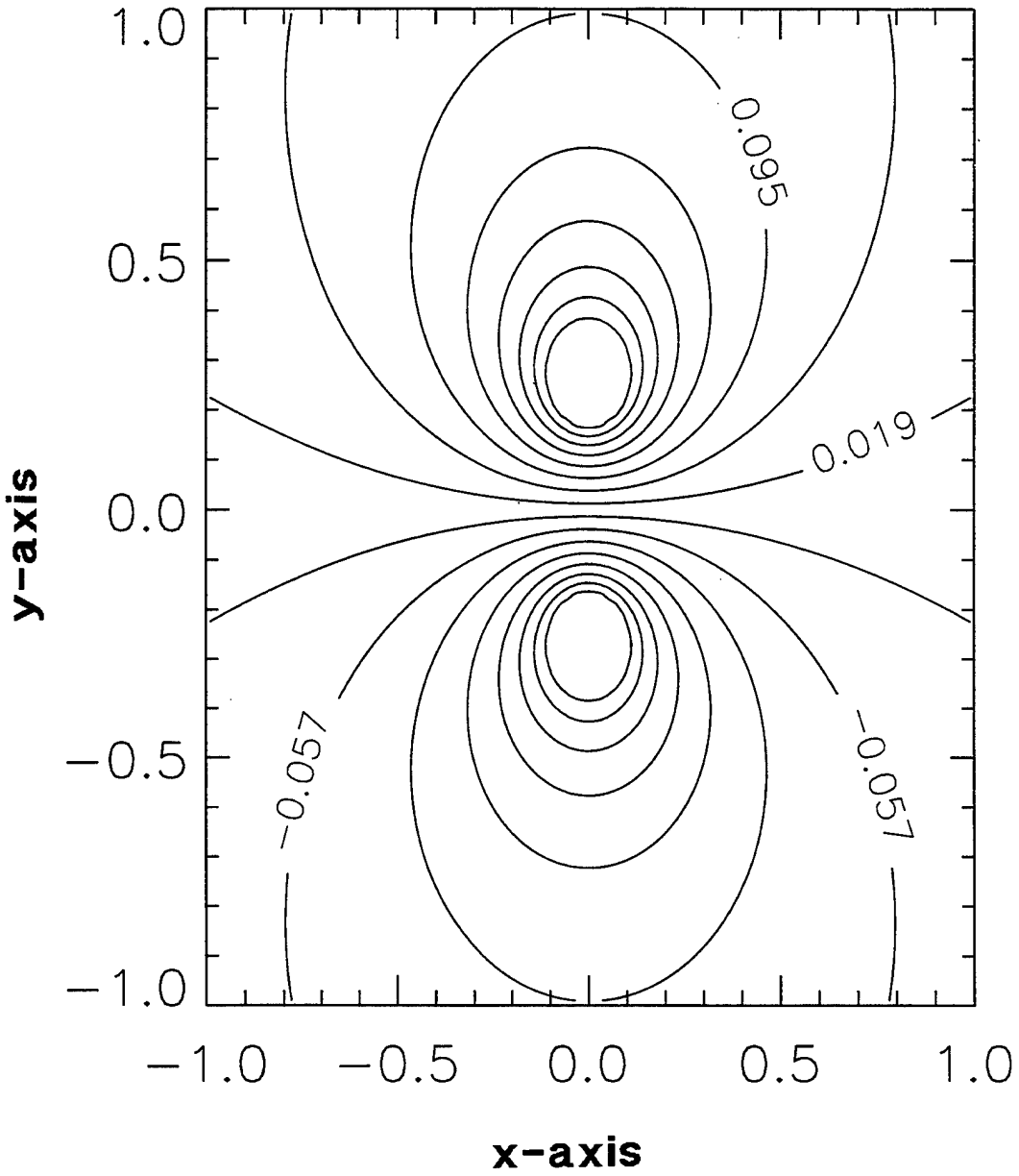

Fig.5

Figure 6. A contour plot of the potential for the case of two parallel wires (really short surface elements) separated by 0.5m and charged to +1V and -1V. Reflective conditions were imposed on the sides at x=1m and -1m using 100 surface elements to resolve the boundary condition. This figure is to be contrasted to Fig. 5. The contours near the charged wires are suppressed for presentation clarity.

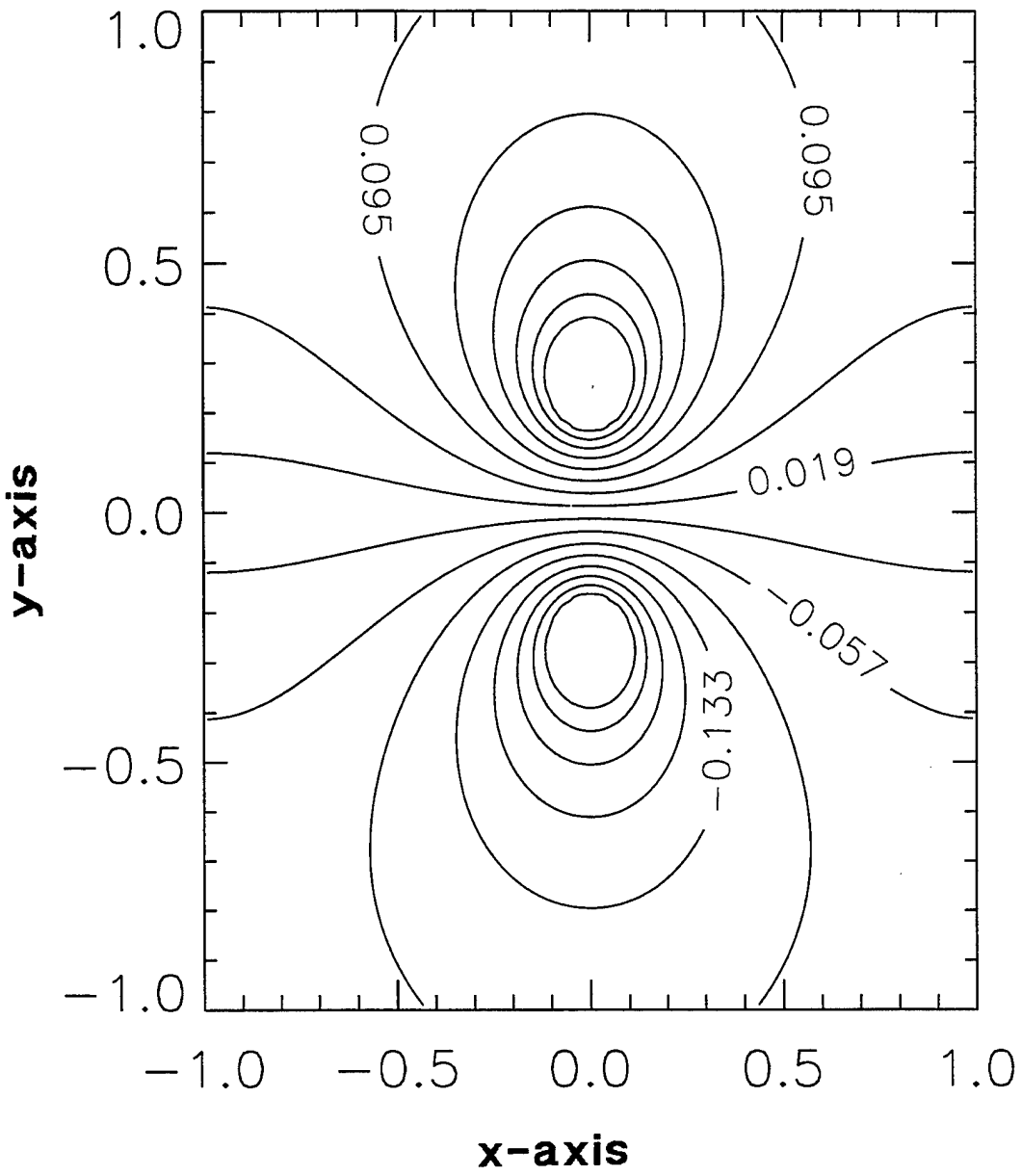
1.0
0.5
0.0
−0.5
−1.0
y-axis
−1.0
−0.5
0.0
0.5
1.0
x-axis
0.095
0.095
0.019
−0.057
−0.133

Fig.6

Figure 7. This is a "wire mesh plot" of the potential due to a space charge distribution whose cross sectional profile is a Gaussian distribution. The evaluation region is a 2m by 2m box. The characteristic radius of the charge is 0.25m and the evaluation grid is 50 by 50. The absolute scale of the potential is arbitrary because of the boundary conditions. The important point here is that the potential evaluation by Eq.(42) and the grid used to compute the space charge in the linear solution, Eq.(20) are the same.

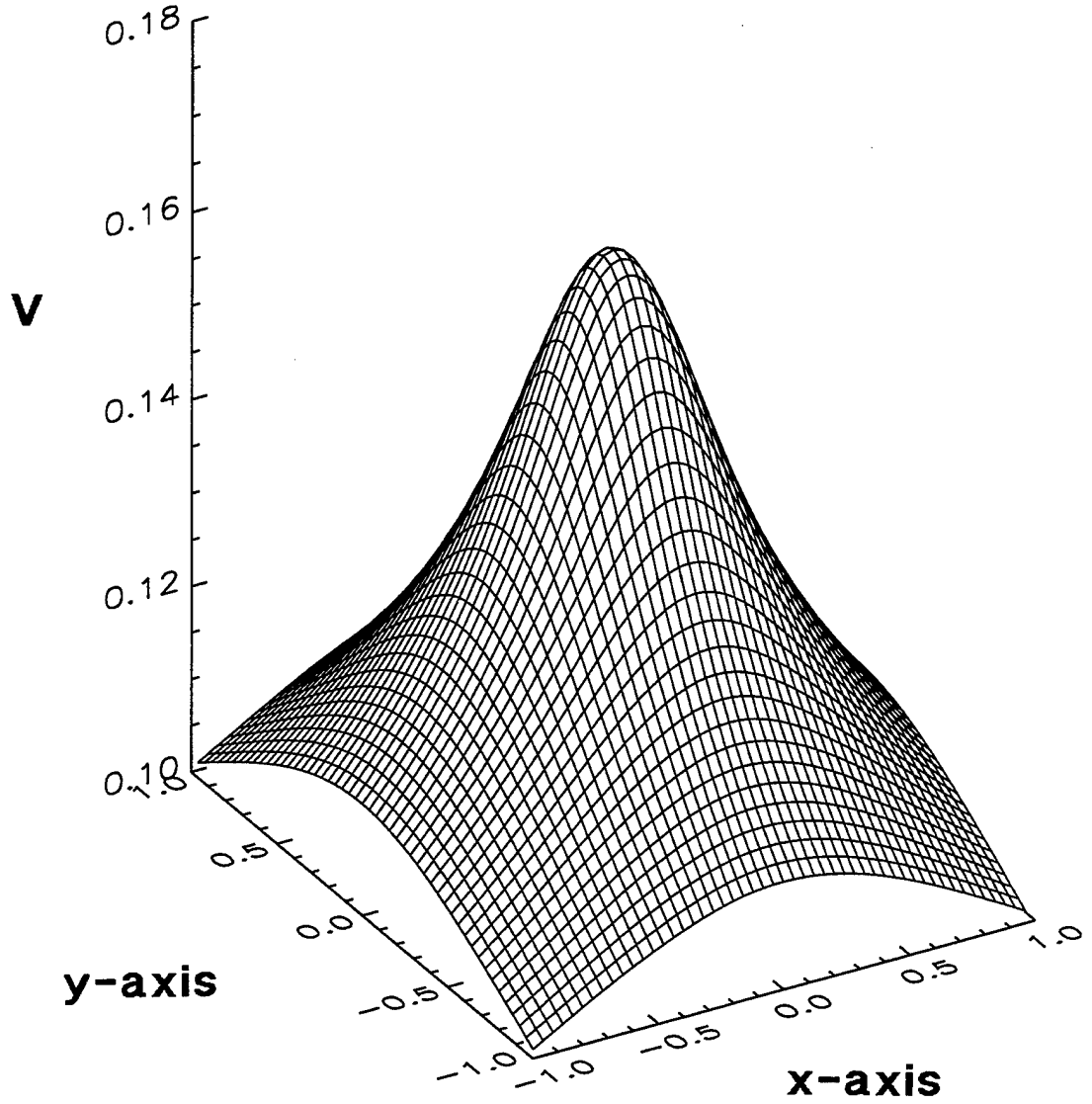

Fig.7

Figure 8. This is a "wire mesh plot" of the y-component of the electric field corresponding to the potential of Fig. 7. The field is due to a space charge distribution whose cross sectional profile is a Gaussian distribution. The evaluation region is a 2m by 2m box. The characteristic radius of the charge is 0.25m and the evaluation grid is 50 by 50, the same as the grid used to represent the volume charge distribution. The important point here is that the field evaluation by Eq.(43) and the grid used to compute the space charge in the linear solution, Eq.(20) are the same.

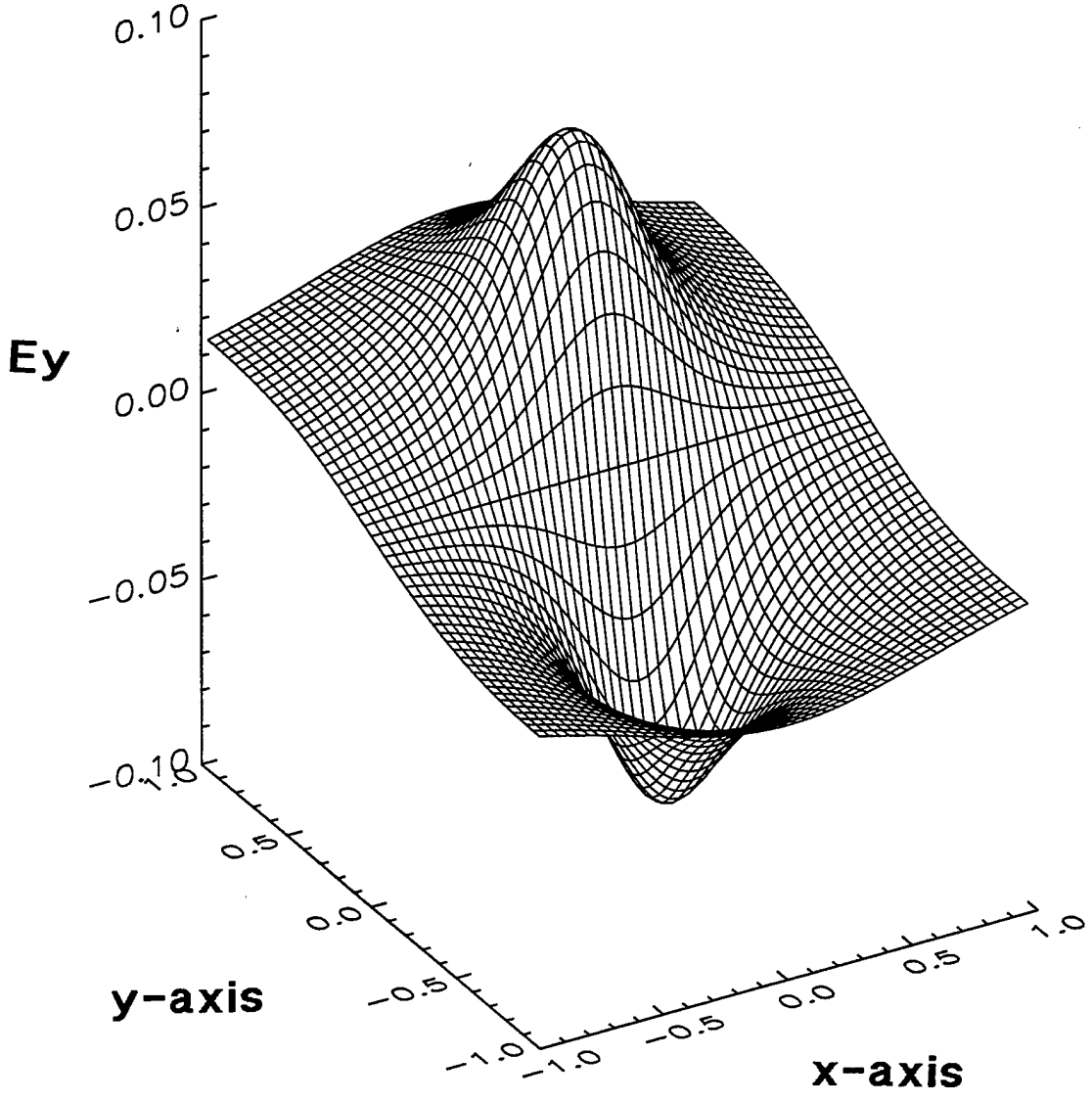

Fig.8

Figure 9. This is the same potential as Fig.7 evaluated and shown on a 10X magnified scale in the center of the charge distribution. The point here is that the potential evaluation by Eq.(42) and the grid used to compute the space charge in the linear solution, Eq.(20) are *not* the same. The potential has some barely discernible ripples which are due to the evaluation of the field *within* the area of the finite elements, which are assumed to be of circular cross section, but are really squares.

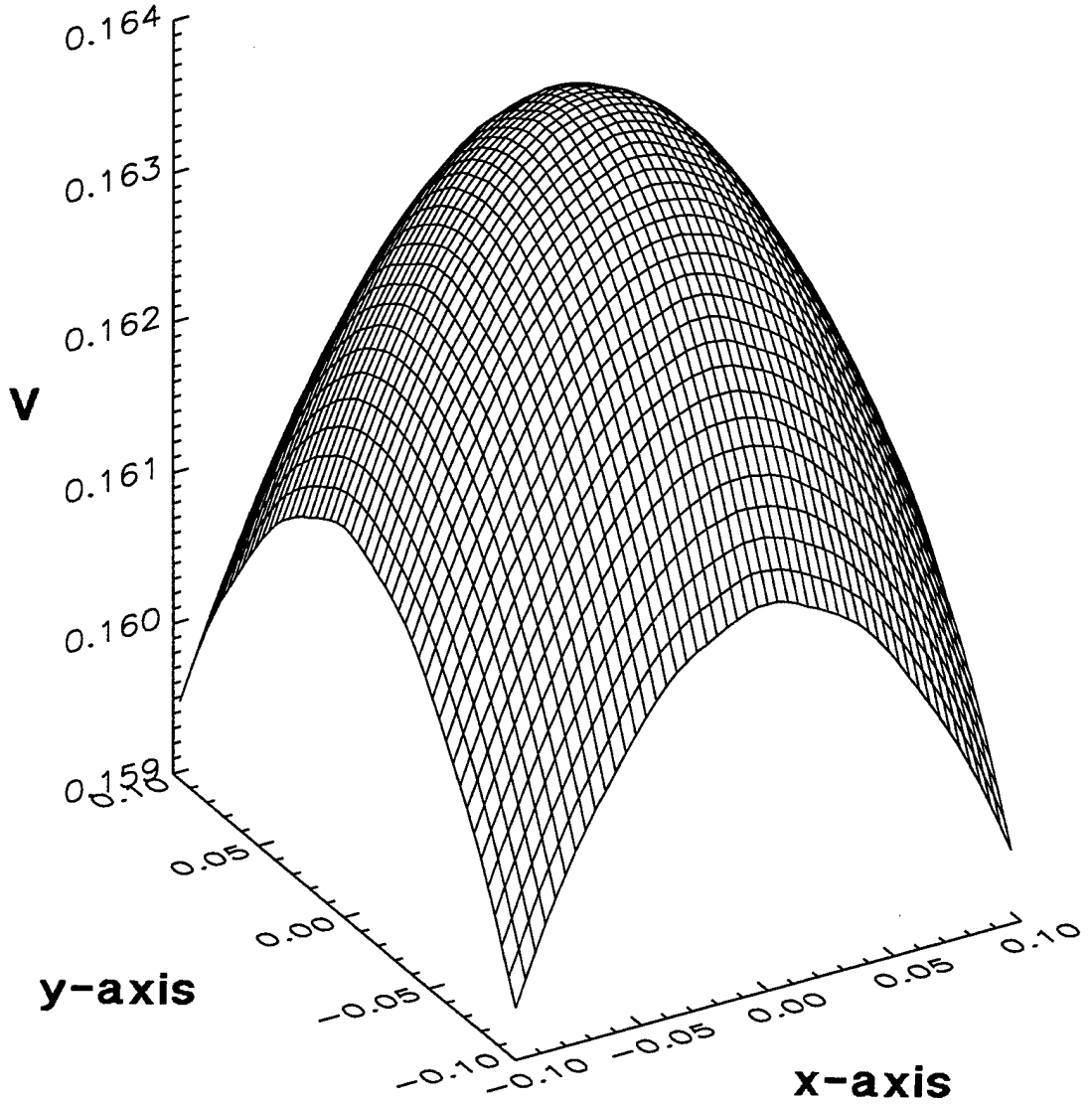
0.164
0.163
0.162
V
0.161
0.160
0.159
0.10
0.05
0.00
−0.05
−0.10
y-axis
−0.10
−0.05
0.00
0.05
0.10
x-axis

Fig.9

Figure 10. This is the same electric field component as shown in Fig.8 evaluated and shown on a 10X magnified scale in the center of the charge distribution. The point here is that the field evaluation by Eq.(43) and the grid used to compute the space charge in the linear solution, Eq.(20) are *not* the same. The field ripples which are due to the evaluation of the field *within* the area of the finite elements, which are assumed to be of circular cross section, but are really squares. Although the ripples are quite obvious, the relative error is on the order of 5%. In the text it is recommended that field evaluations in the presence of significant amount of space charge be done on the *same* grid as used for the representation of the space charge. This avoids the effect shown here and, at least, gives a more eye-pleasing result.

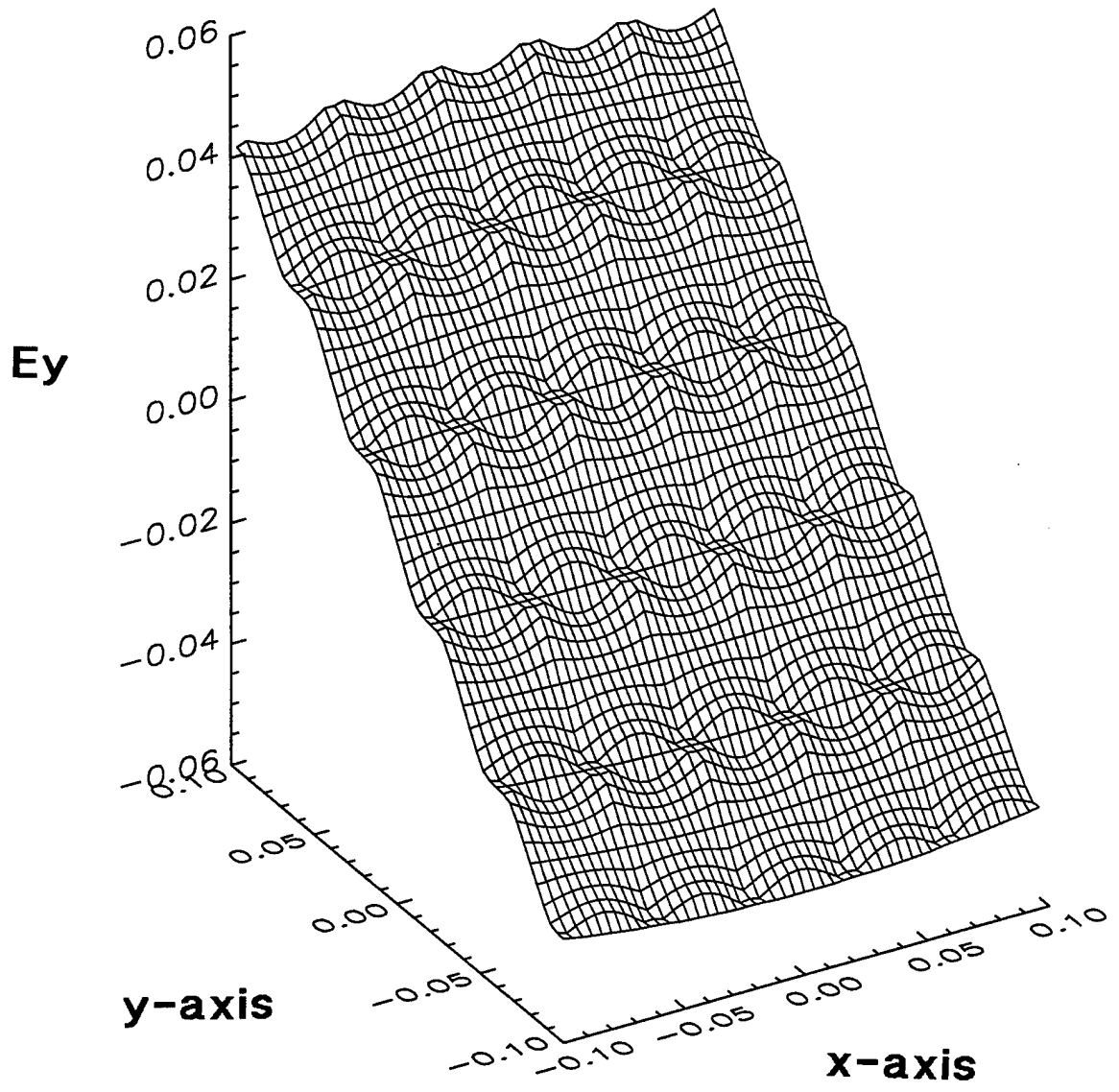
0.06
0.04
0.02
0.00
-0.02
-0.04
-0.06
Ey
0.05
0.00
-0.05
-0.10
y-axis
-0.10
-0.05
0.00
0.05
0.10
x-axis

Fig.10

Figure 11. The potential field within a periodic small feature typical of microelectronic circuitry. The computation volume is a $10\,\mu$m by $10\,\mu$m section with a $1\,\mu$m silicon oxide layer laid on the bottom conducting surface. The x coordinate is periodic. There is a $3\,\mu$m high by $4\,\mu$m wide feature of polysilicon in the center which is also covered with a $1\,\mu$m thick layer of oxide. The polysilicon is a good conductor and is thus at equipotential with zero total charge. The surfaces are all decomposed into element of length $0.1\,\mu$m and the evaluation grid for construction of the surface plots is a 100 by 100 grid with spacing of $0.1\,\mu$m. The voltage of the top (plasma) surface is held at 0V and the bottom is held at -5V. The dielectric oxide regions are visible as "depressions" in the potential field. The polysilicon is the small rectangular region of constant potential.

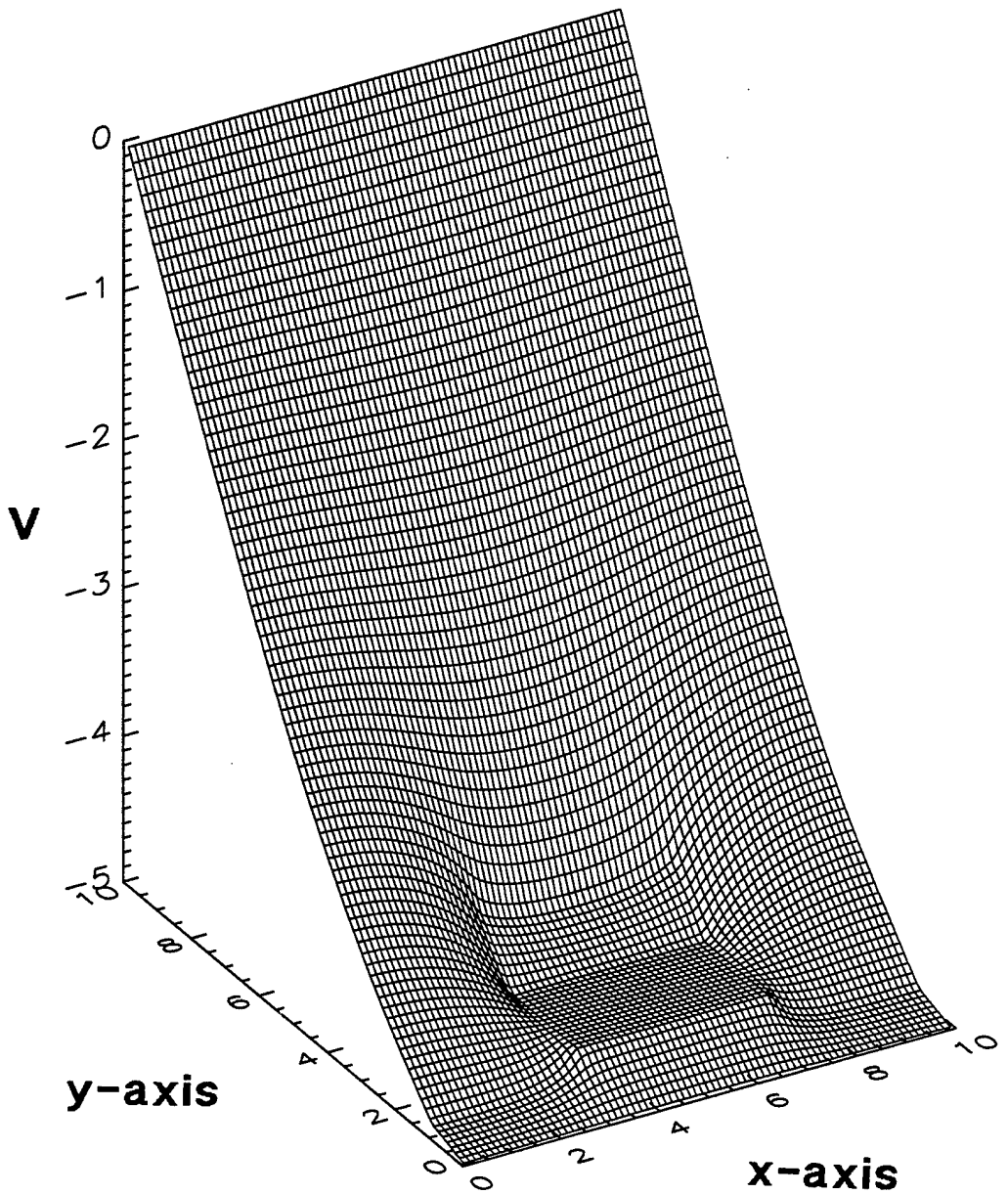

Fig.11

Figure 12. Same as Fig. 11 except that the polysilicon conducting element is allowed to possess a charge (10^{-10}C/m). To be noted is the dramatically changed fields about the element and implications for charged particle motion.

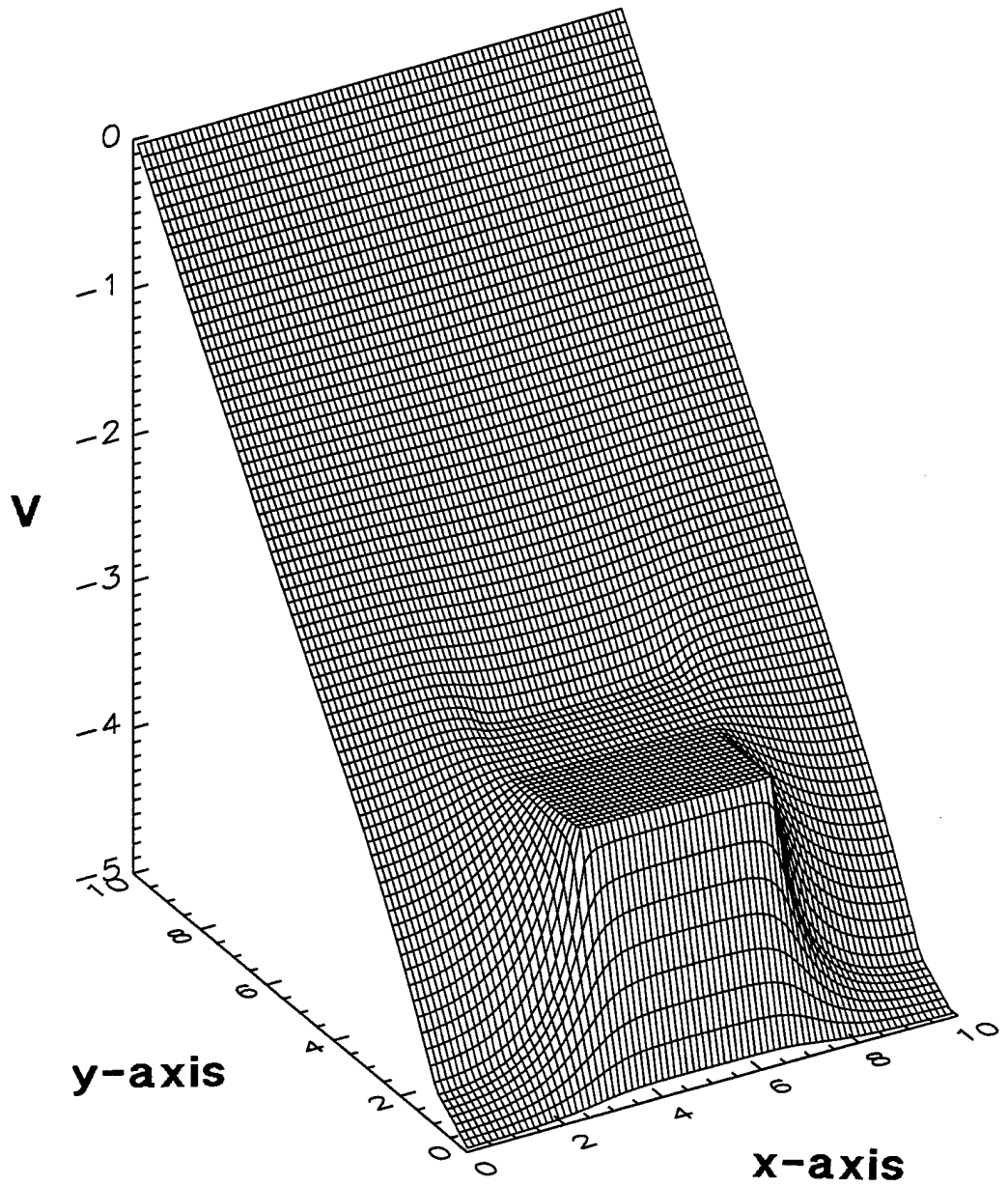

Fig.12

Figure 13. Same as Fig. 11 except that the dielectric oxide top surfaces are allowed to accumulate a surface charge which does not redistribute. To be noted is the changed fields about the surfaces and implications for charged particle motion.

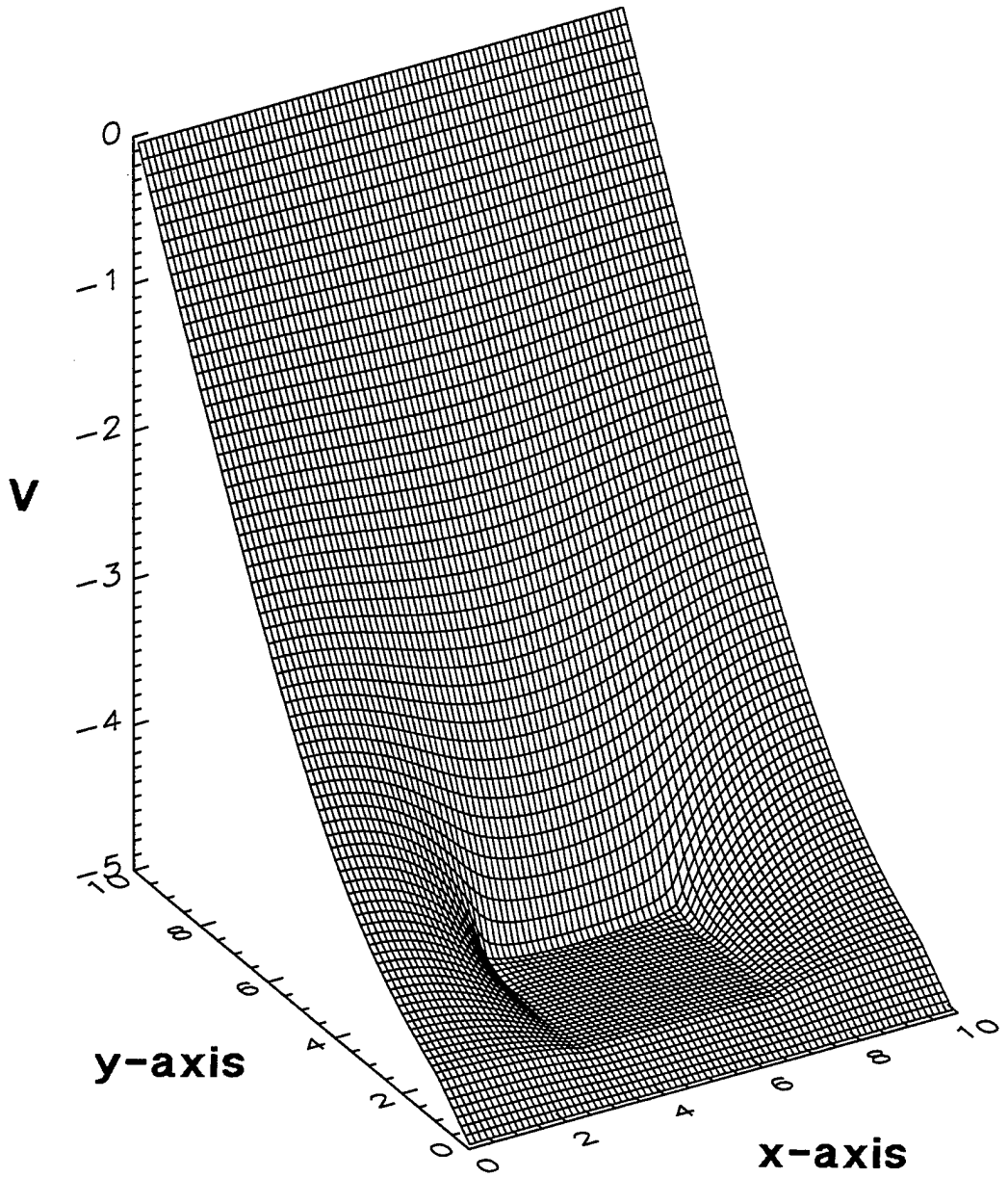

Fig.13

DISTRIBUTION:

1 Professor Demetre J. Economou
Department of Chemical Engineering
University of Houston
Houston, TX 77204-4792

1 Professor Mark Kushner
Electrical and Computer Engineering
University of Illinois
Urbana, IL 61801

1 Professor Robert T. McGrath
Engineering Science & Mechanics Department
227 Hammond Building
Penn State University
University Park, PA 16802

1 Dr. Ramana Veerasingam
MS 0225
Applied Materials Corporation
3100 Bowers Ave., Bldg 2
Santa Clara, CA 95056

1 Robert B. Walker
MS B268
Group T-12,
Los Alamos National Laboratory
Los Alamos, NM 87545

1 MS 0827 Timothy J. Bartel, 9114

1 MS 0516 John P. Brainard, 1564

1 MS 0827 Robert B. Campbell, 9114

1	MS 0827	Mary L. Hudson, 9114
1	MS 1423	Gregory Hebner, 1128
1	MS 0516	Robert J. Koss, 1564
1	MS 1423	Paul A. Miller, 1128
20	MS 1423	Merle E. Riley, 1128
1	MS 1194	Walter W. Simpson, 9573
1	MS 9018	Central Technical Files, 8940-2
2	MS 0899	Technical Library, 4916
2	MS 0619	Review and Approval Desk, 12690 [For DOE/OSTI]

Report Number (14) SAND--98-0537

Publ. Date (11) 199803

Sponsor Code (18) DOE/ER, XF

UC Category (19) UC-401, DOE/ER

DOE